From www.bloodjournal.org by guest on January 11, 2016. For personal use only.

Regular Article

RED CELLS, IRON, AND ERYTHROPOIESIS

Glutathione peroxidase 4 prevents necroptosis in mouse erythroid precursors

Özge Canli,[1] Yasemin B. Alankuş,[2] Sasker Grootjans,[3] Naidu Vegi,[4] Lothar Hültner,[5] Philipp S. Hoppe,[6] Timm Schroeder,[6] Peter Vandenabeele,[3] Georg W. Bornkamm,[5] and Florian R. Greten[1]

[1]Institute for Tumor Biology and Experimental Therapy, Georg-Speyer-Haus, Frankfurt, Germany; [2]Institute of Clinical Chemistry, Klinikum rechts der Isar, Technical University Munich, Munich, Germany; [3]Department of Molecular Biomedical Research, VIB, VIB-Ghent University, Ghent (Zwijnaarde), Belgium; [4]Institute of Experimental Cancer Research, Comprehensive Cancer Center and University Hospital Ulm, Ulm, Germany; [5]Institute of Clinical Molecular Biology and Tumor Genetics, Helmholtz Zentrum München, Munich, Germany; and [6]Department of Biosystems Science and Engineering, Swiss Federal Institute of Technology in Zurich, Basel, Switzerland

Key Points

- Gpx4 is essential for preventing anemia in mice via inhibiting RIP3-dependent necroptosis in erythroid precursor cells.
- ROS accumulation and lipid peroxidation in erythroid precursor cells trigger receptor-independent activation of necroptosis.

Maintaining cellular redox balance is vital for cell survival and tissue homoeostasis because imbalanced production of reactive oxygen species (ROS) may lead to oxidative stress and cell death. The antioxidant enzyme glutathione peroxidase 4 (Gpx4) is a key regulator of oxidative stress–induced cell death. We show that mice with deletion of *Gpx4* in hematopoietic cells develop anemia and that Gpx4 is essential for preventing receptor-interacting protein 3 (RIP3)-dependent necroptosis in erythroid precursor cells. Absence of *Gpx4* leads to functional inactivation of caspase 8 by glutathionylation, resulting in necroptosis, which occurs independently of tumor necrosis factor α activation. Although genetic ablation of *Rip3* normalizes reticulocyte maturation and prevents anemia, ROS accumulation and lipid peroxidation in *Gpx4*-deficient cells remain high. Our results demonstrate that ROS and lipid hydroperoxides function as not-yet-recognized unconventional upstream signaling activators of RIP3-dependent necroptosis. (*Blood*. 2016;127(1):139-148)

Introduction

Oxidative stress is defined as the imbalance in cellular redox in favor of the oxidants. At low levels, reactive oxygen species (ROS) act as second messengers,[1] whereas at high levels, they can damage organelles and DNA and can induce programmed cell death such as apoptosis and necroptosis.[2,3] Increased oxidative stress plays a crucial role in a variety of pathological conditions, including cancer, degenerative diseases, and aging.

Due to their physiological function in oxygen transport, oxygen-loaded erythrocytes are under constant oxidative stress. Thus, erythrocytes are equipped with a battery of antioxidant enzymes that supports dismutation of superoxide radicals, detoxification of hydrogen and lipid peroxides, and maintenance of a reducing intracellular milieu (eg, superoxide dismutase 1 and 2, catalase, glutathione peroxidase 1, peroxiredoxin I and II, and glutathione-synthesizing enzymes). Mutations in many of these genes in humans[4] and disruption of the genes in mice cause hemolytic anemia.[5-7] Similarly, selenium deficiency leads to anemia in vertebrates,[8] yet the contribution of individual selenoproteins hereto is still unknown. Glutathione peroxidase 4 (Gpx4) has a very high rank within the so-called selenium hierarchy among mammalian selenoproteins, which is determined based on the expression level of a selenoprotein under selenium deficiency due to its stable expression even when selenium is rare, thus indicating a strong dependence on this enzyme.[9] Of importance, Gpx4 is the only glutathione peroxidase known to be essential for embryonic development.[10,11] Moreover, Gpx4 controls caspase-independent cell death in neurons,[12] photoreceptor cells,[13] and T cells.[14]

Ferroptosis is a nonapoptotic form of cell death involving the production of iron-dependent ROS.[15] It was recently noted that the oncogenic RAS-selective lethal small molecule erastin triggers ferroptosis via inhibiting cysteine uptake by the cysteine/glutamate antiporter, leading to iron-dependent accumulation of lethal lipid ROS and eventually to ferroptotic cell death, which is morphologically, biochemically, and genetically distinct from apoptosis and necrosis. Gpx4 was later identified as an essential regulator of ferroptotic cancer cell death.[16] In addition to the cancer cells, *Gpx4* depletion leads to massive cell death through the induction of lipid peroxidation and ferroptotic machinery in renal tubular epithelia[17] and in T cells.[14]

In addition to apoptosis and ferroptosis, several other forms of programmed cell death have been described, including poly(adenosine 5′-diphosphate ribose) polymerase (PARP)1-dependent and apoptosis-inducing factor 1–dependent parthanatos, caspase 1–dependent pyroptosis, and receptor-interacting protein (RIP) 1–dependent necroptosis.[15,18-21] Necroptosis can be triggered by ligation of death

Submitted June 26, 2015; accepted October 3, 2015. Prepublished online as *Blood* First Edition paper, October 13, 2015; DOI 10.1182/blood-2015-06-654194.

The online version of this article contains a data supplement.

There is an Inside *Blood* Commentary on this article in this issue.

The publication costs of this article were defrayed in part by page charge payment. Therefore, and solely to indicate this fact, this article is hereby marked "advertisement" in accordance with 18 USC section 1734.

© 2016 by The American Society of Hematology

From www.bloodjournal.org by guest on January 11, 2016. For personal use only.

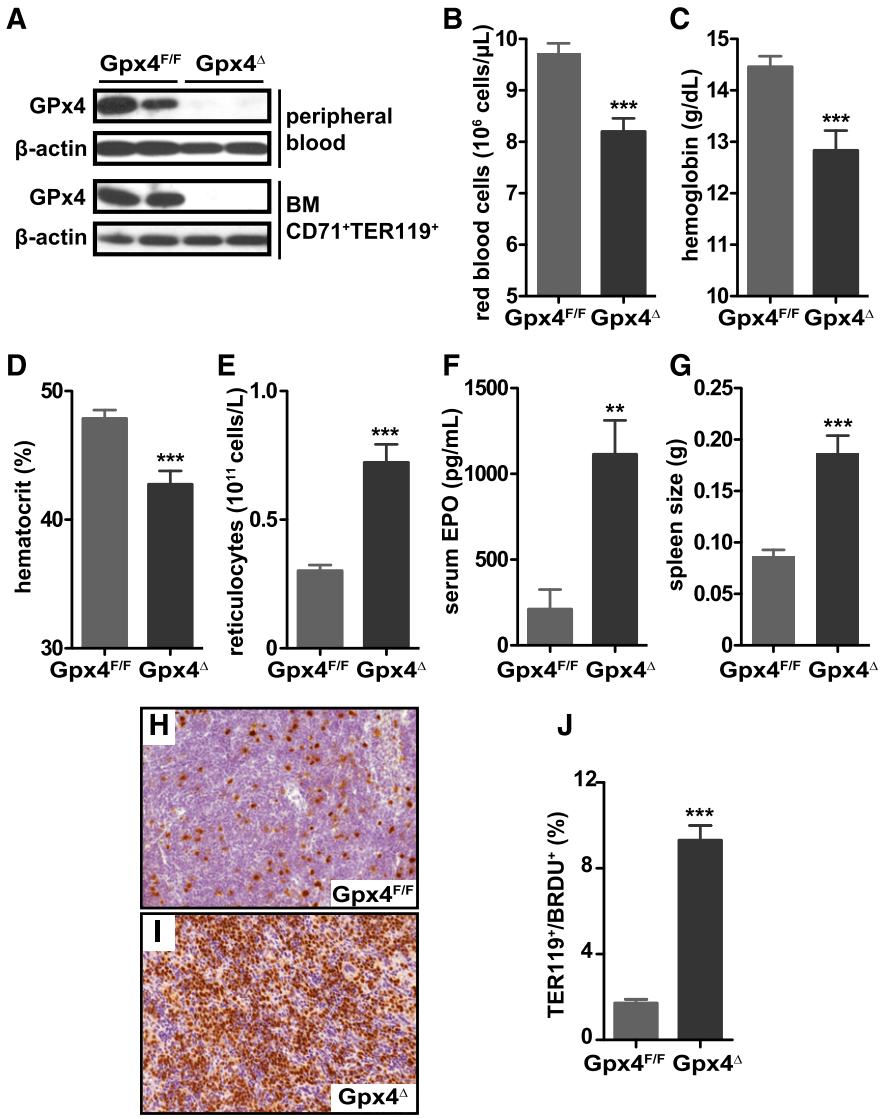

Figure 1. Loss of *Gpx4* in hematopoietic cells induces anemia that is compensated by increased erythropoiesis. (A) Immunoblot analysis of Gpx4 in peripheral erythrocytes (TER119$^+$) and bone marrow erythroid progenitors (CD71$^+$/TER119$^+$). Red blood cell counts (B), hemoglobin levels (C), and hematocrit (D) are decreased in *Gpx4*$^{\Delta}$ mice, whereas the number of reticulocytes is increased (E). Data are mean ± SE; n ≥ 20. Elevated serum EPO levels (F) and enlarged spleens (G) in *Gpx4*$^{\Delta}$ mice. Data are mean ± SE; n ≥ 10. (H-I) Immunohistochemistry staining of BrdU incorporation in the spleen and nuclear counterstain hematoxylin. Image acquisition was performed using a Zeiss Axio Imager M2 with a 20×/0.5 EC Plan Neofluar objective (magnification ×200). (J) Quantification of splenic BrdU$^+$/TER119$^+$ cells determined by flow cytometry. Data are mean ± SE; n ≥ 3. $^{**}P < .01$, $^{***}P < .001$ by Student *t* test. BM, bone marrow; SE, standard error.

receptors such as CD95, tumor necrosis factor (TNF) receptor 1 and 2 (TNFR1 and 2), as well as TNF-related apoptosis-inducing ligand receptor 1 and 2.[22] The best-characterized pathway inducing necroptosis involves TNFR1 ligation and depends on the activity of caspase 8, which acts as the molecular switch between apoptosis and necroptosis. In the case of caspase 8 inhibition, the necrosome, a multiprotein complex containing RIP1 and RIP3, is formed and activated, culminating in the production of mitochondrial ROS and the generation of lipid peroxides as an essential prerequisite for execution of TNF-dependent necrosis.[22,23] So far, mitochondrial ROS production has been described only as a downstream effector mechanism upon necrosome activation. However, direct evidence that ROS could lead to activation of RIP1/RIP3 even as part of a positive feedback loop is lacking. Several important physiological roles of necroptosis were demonstrated by recent studies showing that caspase 8 or Fas-associated protein with death domain (FADD) deficiency causes embryonic lethality and triggers inflammation in vivo by sensitizing cells to RIP3-mediated necroptosis.[24-28] Both caspase 8 and FADD knockout mice strains die at the same embryonic stage with a similar phenotype. Cell death observed in the absence of caspase 8 is inhibited upon the additional deletion of *Rip3*, suggesting that caspase 8 inhibits RIP3-mediated necroptosis.[24,25,29]

Although Gpx4 has been identified as an important enzyme for the homeostasis of many cell types, no studies have so far linked Gpx4 to the red blood system. In this study, we addressed the function of Gpx4 in the erythroid lineage and provide evidence that Gpx4 is essential for erythrocyte homeostasis and for prevention of RIP3-dependent necroptosis independently of death receptor engagement.

Methods

Mice

Gpx4$^{F/F}$ mice were crossed to *Mx1-Cre* or *Rosa26-CreER*^{T2} mice and kept on a mixed genetic background. Rip3$^{-/-}$ mice[30] were crossed to *Mx1-Cre/Gpx4*$^{F/F}$ mice. Deletion of *Gpx4* was induced by a single intraperitoneal (IP) injection of 250 μg polyinosinic-polycytidylic acid (poly[I:C]; Sigma) dissolved in water. Vitamin E–deficient diet was purchased from Ssniff (E15791-147). In adoptive transfer experiments, recipient mice were lethally irradiated (9 Gy) and injected with 1 × 10^6 donor bone marrow cells into the tail vein. For complete blood counts and flow cytometry analysis, blood was collected from the facial or tail vein in dipotassium EDTA collection tubes (Sarstedt), and measurements were

From www.bloodjournal.org by guest on January 11, 2016. For personal use only.

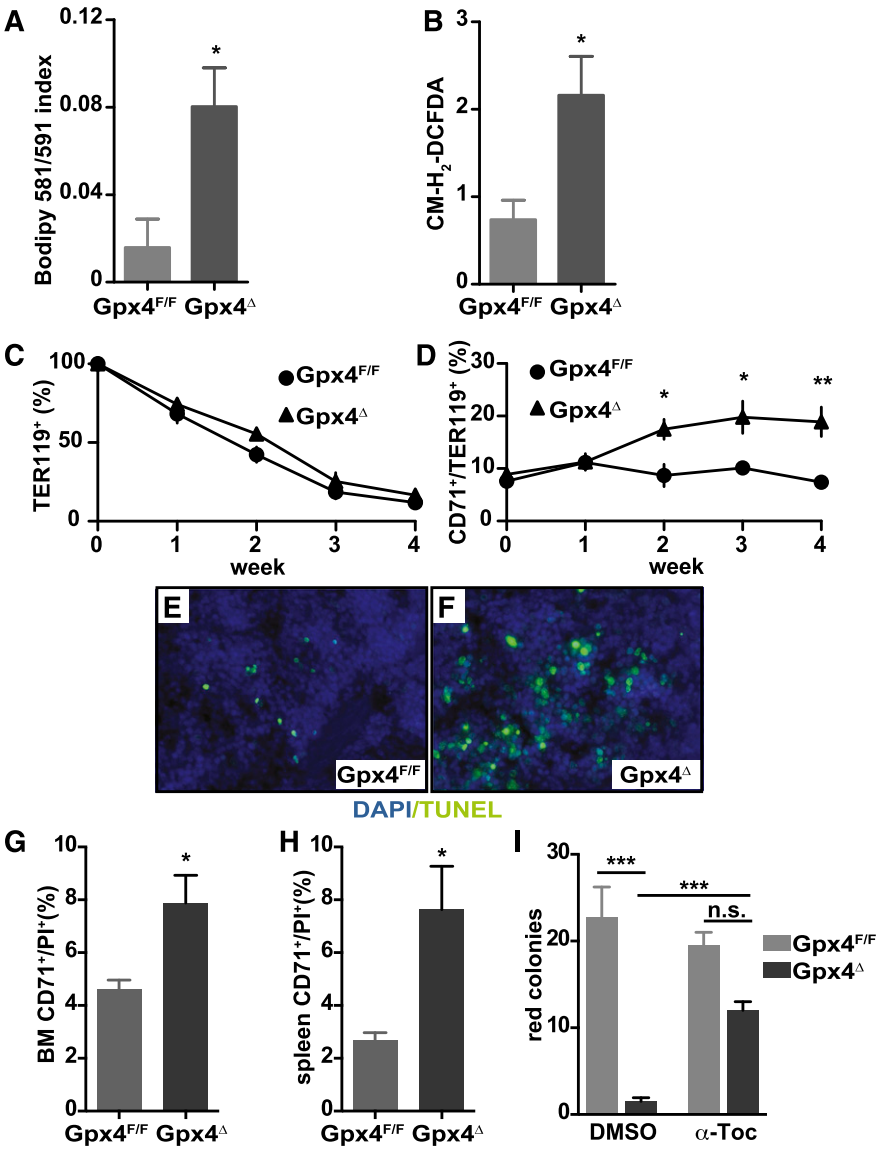

Figure 2. Increased lipid peroxidation and oxidative stress in *Gpx4*$^{\Delta}$ erythroid cells does not impair their life span in the periphery. (A) Measurement of lipid peroxidation in unchallenged peripheral TER119^{+} erythrocytes using the lipophilic redox-sensitive dye BODIPY 581/591, which upon oxidation, shifts its fluorescence from red to green. Data are mean ± SE; n ≥ 7. (B) ROS in unchallenged peripheral TER119^{+} erythrocytes using the redox-sensitive dye 5-(and-6)-chloromethyl-2′,7′-dichlorodihydrofluorescein diacetate, acetyl ester (CM-H_2-DCFDA) (n ≥ 7). (C) Survival of biotin-labeled peripheral TER119^{+} erythrocytes. Data are mean ± SE; n ≥ 6. (D) Increased number of peripheral CD71^{+}/TER119^{+} reticulocytes in *Gpx4*$^{\Delta}$ mice within the first 4 weeks after poly(I:C) administration. Data are mean ± SE; n ≥ 5. (E-F) Representative images of TUNEL assay in spleen sections and 4,6 diamidino-2-phenylindole (DAPI) as a counterstain showing increased cell death in *Gpx4*$^{\Delta}$ mice. Image acquisition was performed using a Zeiss Axio Imager M2 with 40×/0.95 korr Apochromat objective (magnification ×400). Flow cytometry analysis using PI to determine the number of nonviable CD71^{+} cells in bone marrow (G) and in spleen (H). Data are mean ± SE; n ≥ 3. (I) Formation of *o*-dianisidine–positive erythroid colonies from bone marrow in methylcellulose semisolid media. Red colony formation of *Gpx4*$^{\Delta}$ bone marrow cells could be rescued by addition of α-tocopherol to the medium. Data are mean ± SE; n ≥ 3. **P* < .05, ***P* < .01, ****P* < .001 by Student *t* test. α-Toc, α-tocopherol; n.s., not significant; PI, propidium iodide.

performed via Sysmex-XT-2000i. For biotin-labeling experiments, mice were injected daily with 1 mg of IV biotinyl-N-hydroxysuccinimide ester (203118; Calbiochem) for 3 days starting on the day of poly(I:C) administration. Ten microliters of blood was used for flow cytometry analysis. Starting 2 weeks after poly(I:C) administration, 50 μg of anti-CD95L neutralizing antibody (555291; BD Pharmingen) and 5 mg/kg of olaparib (Selleckchem) were administered by IP injection every 3 days. All animal procedures were performed in accordance with institutional guidelines.

In vitro differentiation of erythroid cells

Mouse erythroid cultures were prepared as described previously.[31] Lineage-negative bone marrow cells were prepared using biotin-labeled lineage cell detection cocktail (130-092-613; Miltenyi Biotec) and streptavidin microbeads (130-048-101; Miltenyi Biotec) according to the manufacturer's instructions. Purified cells were seeded in fibronectin-coated plates (Corning) in Iscove modified Dulbecco medium (12440053; Gibco) containing 15% fetal bovine serum, penicillin/streptomycin (Gibco), 200 μg/mL of holotransferrin (T0665; Sigma), 10 μg/mL of recombinant human insulin (I9278; Sigma), and 2 units/mL of erythropoietin (EPO; 287-TC-500; R&D Systems). One day later, the medium was changed to Iscove modified Dulbecco medium with 15% fetal bovine serum and penicillin/streptomycin supplemented with either 1 μM 4-hydroxytamoxifen (4-OHT; Sigma) to induce the deletion of *Gpx4* or 70% ethanol as control. For the inhibitor experiments, all inhibitors were added to the medium together with the 4-OHT. Human recombinant TNF-α (R&S Systems) was used at 100 ng/mL, the transforming growth factor β–activated kinase (TAK) 1 inhibitor (TAKi) 5Z-7-oxozeaenol (Sigma) at 1 μM, caspase inhibitor 1 (zVAD; Calbiochem) at 50 μM, the TNF antagonist etanercept at 1 μM, dithiothreitol (DTT; Sigma) at 25 μM, necrostatin 1 (nec-1; Calbiochem) at 25 μM, ferrostatin 1 (Fer-1; Calbiochem) at 1 μM, liproxstatin 1 (Lip-1; Selleckchem) at 1 μM, deferoxamine (DFO; Sigma) at 1 mM, erastin (Sigma) at 10 μM, and Ras synthetic lethality molecule 3 (InterBioScreen) at 5 μM. Cell viability was determined via trypan blue exclusion count.

Flow cytometry and cell separation

For flow cytometric analysis, cells were stained using the fluorophore-conjugated antibodies anti-TER119 (eBiosciences) and anti-CD71 (eBiosciences) (0.1-0.2 μg/10^6 cells) in fluorescence-activated cell-sorting buffer (2% fetal calf serum/2 mM EDTA/phosphate-buffered saline). A total of 10^6 cells were labeled for 30 minutes at 37°C with the redox-sensitive fluorescent probe 5-(and-6)-chloromethyl-2′,7′-dichlorodihydrofluorescein diacetate, acetyl ester (Invitrogen) (1 μM) to measure the cellular ROS and with C11-BODIPY 581/591 (2 μM) to measure cellular lipid peroxidation before surface marker stainings. Annexin V staining was performed according to the manufacturer's instructions (BD Pharmingen). To determine splenocyte proliferation, mice were administered

From www.bloodjournal.org by guest on January 11, 2016. For personal use only.

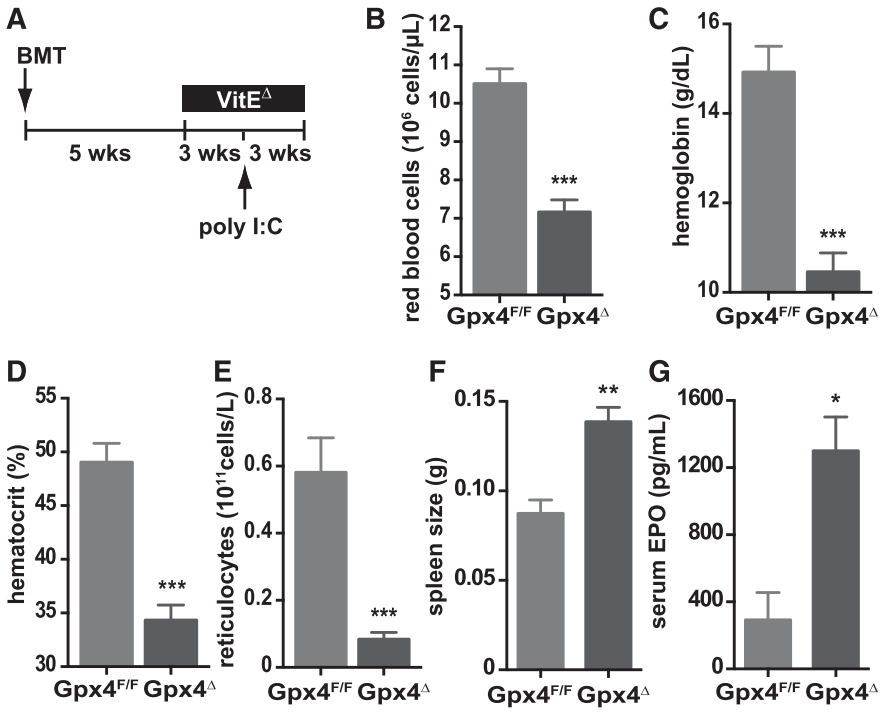

Figure 3. Increased erythropoiesis in *Gpx4*$^{\Delta}$ mice depends on vitamin E. (A) Schematic overview of treatment: bone marrow from *Gpx4*$^{F/F}$ or *Mx1-Cre/Gpx4*$^{F/F}$ mice was transplanted (BMT) into wild-type recipients; mice were kept on a vitamin E–depleted diet (VitE$^{\Delta}$) after the recovery; and deletion was induced by poly(I:C). Red blood cell counts (B), hemoglobin levels (C), hematocrit (D), and reticulocyte counts (E). Data are mean ± SE; n ≥ 4. Enlarged spleens (F) and elevated serum EPO levels (G) in transplanted mice. Data are mean ± SE; n ≥ 6. ***$P < .001$, **$P < .01$, *$P < .05$ by Student *t* test.

100 mg/kg of 5-bromo-2′-deoxyuridine (BrdU) by IP injection 4 hours before being euthanized, and splenocytes were subjected to BrdU assay (BD Pharmingen). Cell separations were done using magnetic beads according to the manufacturer's instructions (Miltenyi Biotec).

Immunohistochemical analysis

Standard immunohistochemical procedures were performed using the following antibodies: anti-BrdU (MCA2060; AbD Serotec) and anti-phospho-Histone H2A.X (2577; Cell Signaling). Terminal deoxynucleotidyl transferase deoxyuridine triphosphate nick-end labeling (TUNEL) assay was performed with the ApoAlert DNA Fragmentation Assay Kit (Clontech). Briefly, tissues were treated with proteinase K, incubated with terminal deoxynucleotidyl transferase enzyme mix, and mounted in medium containing 4,6 diamidino-2-phenylindole. Image acquisition was performed 2 hours later using a Zeiss Axio Imager M2 with a 20×/0.5 EC Plan Neofluar or a 40×/0.95 korr Apochromat objective and AxioVision software.

Protein analysis

Proteins lysates were prepared using lysis buffer (50 mM Tris (pH 7.5), 250 mM sodium chloride, 30 mM EDTA, 30 mM EGTA, 25 mM sodium pyrophosphate, 1% Triton-X 100, 0.5% nonylphenoxypolyethoxyethanol, 10% glycerol, and protease and phosphatase inhibitors [Roche]). The following antibodies were used for immunoblot analysis: anti-RIP1 (610459; BD Biosciences), anti-RIP3 (62344; Abcam), anti–β-actin (Sigma-Aldrich), anti-Gpx4 (ab125066; Abcam), anti-FADD (M-19, sc-6036; Santa Cruz Biotechnology), and anti–caspase 8 (MAB3429; Abnova). Immunoprecipitation experiments were performed with the standard procedures using anti–caspase 8 (rabbit polyclonal), with 30 minutes of antibody binding to the protein A sepharose beads (GE Healthcare), followed by overnight incubation with protein lysates.

For glutathionylation analysis, cells were labeled with biotin-labeled glutathione ethylester (BioGEE; Invitrogen) for 30 minutes at 37°C. The cells were lysed in BioGEE lysis buffer containing 50 mM Tris (pH 7.5), 250 mM sodium chloride, 30 mM EDTA, 30 mM EGTA, 25 mM sodium pyrophosphate, 1% triton-X 100, 0.5% nonylphenoxypolyethoxyethanol, and 10% glycerol. Biotinylated proteins were precipitated from cell lysates with streptavidin agarose beads (Thermo Scientific) for 20 minutes and were eluted with BioGEE lysis buffer containing 10 mM DTT. Samples were boiled for 5 minutes at 95°C in Laemmli buffer and subjected to immunoblot analysis. Reduced glutathione (GSH) measurements were done using the Glutathione Assay Kit II (Calbiochem) according to the manufacturer's instructions, with or without 2-vinylpyridine for the detection of oxidized glutathione (GSSG) or total GSH, respectively. Absorbance at 405 nm was detected, and the concentrations were calculated based on the corresponding standards. EPO (Mep00; R&D Systems), interleukin 6 (DY406; R&D Systems), and anti–double-stranded DNA (Alpha Diagnostic International) enzyme-linked immunosorbent assays were performed according to the manufacturers' instructions using 50 μL of serum.

Results

Loss of Gpx4 in hematopoietic cells induces compensated anemia

To functionally examine the consequences of *Gpx4* deficiency in the erythroid lineage regarding uncontrolled ROS accumulation and lipid peroxidation and their possible effects on cell death, we crossed floxed *Gpx4* (*Gpx4*$^{F/F}$) mice to *Mx1-Cre* transgenic mice[32] to generate *Mx1-Cre/Gpx4*$^{F/F}$ (hereafter referred to as *Gpx4*$^{\Delta}$) mice. Deletion of *Gpx4* in hematopoietic cells was induced by a single IP poly(I:C) injection. Absence of Gpx4 in CD71^{+}/Ter119^{+} bone marrow erythroblasts and in peripheral mature CD71^{-}/Ter119^{+} erythrocytes was confirmed by immunoblot analysis (Figure 1A). Loss of *Gpx4* in hematopoietic cells led to a moderate yet significant decrease in red blood cell counts, hemoglobin levels, and hematocrit 4 weeks after poly(I:C) administration (Figure 1B-D). In contrast, reticulocyte counts increased more than twofold, indicating a compensatory increase of erythropoiesis (Figure 1E). In parallel, serum EPO levels were more than fivefold elevated (Figure 1F). Moreover, increased spleen weight (Figure 1G) and elevated number of proliferative CD71^{+}/Ter119^{+} erythroblasts in the spleen (Figure 1H-J) supported the notion that anemia in *Gpx4*$^{\Delta}$ mice was highly compensated by extramedullary erythropoiesis. The percentage of CD71^{+} cells is

From www.bloodjournal.org by guest on January 11, 2016. For personal use only.

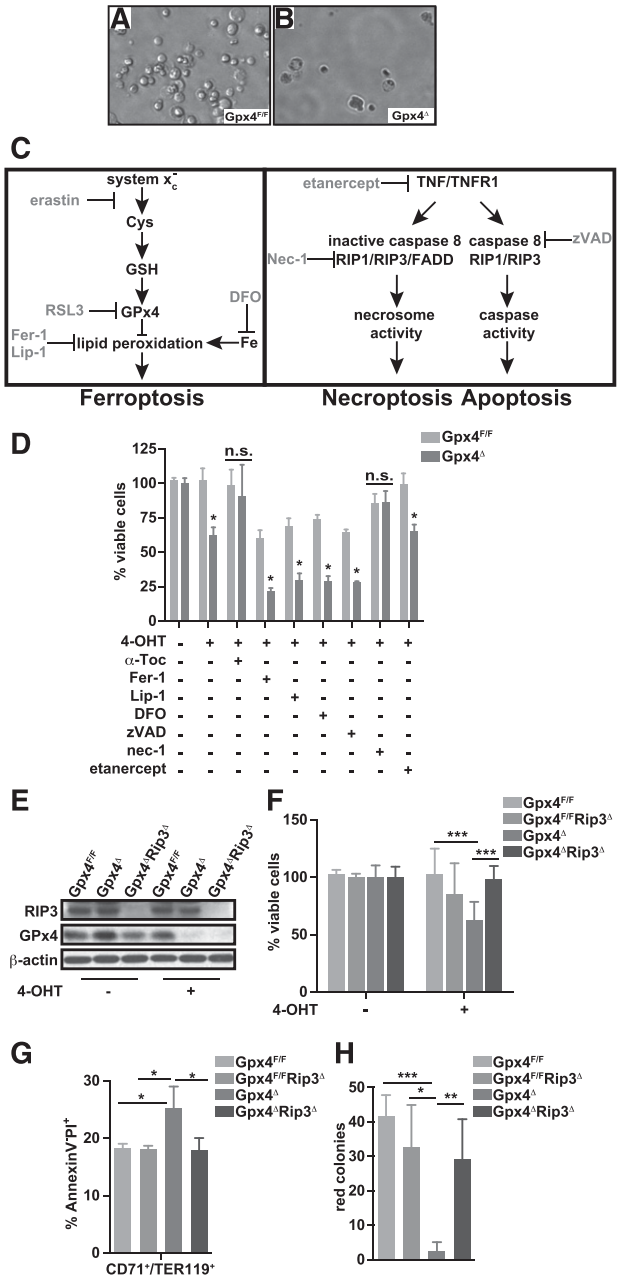

Figure 4. RIP3-dependent necroptosis, but not ferroptosis, causes cell death in *Gpx4*-deficient erythroid progenitor cells. Erythroid cells were differentiated in vitro from *Gpx4*$^{F/F}$ and *Rosa26-Cre*ER^{T2}/*Gpx4*$^{F/F}$ bone marrow, and deletion was induced by 4-OHT after 24 hours of culture in the presence of EPO. Microscopic images of in vitro–differentiated erythroid cells from *Gpx4*$^{F/F}$ (A) and *Rosa26-Cre*ER^{T2}/*Gpx4*$^{F/F}$ (*Gpx4*$^{\Delta}$) (B) bone marrow 48 hours after the induction of deletion with tamoxifen. (C) Schematic illustration of programmed cell death pathways. Ferroptosis (left) is triggered by an iron-dependent accumulation of lethal ROS and lipid peroxides in cells, which can be inhibited via iron (Fe) chelators such as DFO. Ferroptosis can be induced by erastin, which inhibits cellular cysteine (Cys) uptake and thus limits the production of intracellular GSH, or by Ras synthetic lethality molecule 3 (RSL3) via inhibition of Gpx4, leading to increased lipid peroxidation and ROS accumulation. Fer-1 and Lip-1 inhibit ferroptosis via inhibiting the lipid peroxidation. Apoptosis and necroptosis (right) are mainly regulated via TNFR1 signaling. Upon TNF binding, TNFR1 undergoes a conformational change, activating 2 possible cell death execution mechanisms: caspase-dependent or caspase-independent. Normally, caspase 8 triggers apoptosis by activating the classical caspase cascade. It also cleaves, and hence inactivates, RIP1 and RIP3. If caspase 8 is inhibited (eg, via zVAD), phosphorylated RIP1 and RIP3 engage the effector mechanisms of necroptosis. (D) Percentage of viable in vitro–differentiated erythroid cells counted via trypan blue exclusion 48 hours after the induction of deletion in the presence of α-tocopherol (the most prominent member of the vitamin E family), the ferroptosis inhibitors Fer-1 and Lip-1, the iron chelator DFO, the pan-caspase inhibitor zVAD, the necroptosis inhibitor nec-1, or recombinant soluble TNFR2 (etanercept). Data are mean ± SE; n ≥ 6; **P* < .05 by Student *t* test. (E) Absence of Gpx4 and RIP3 is verified by immunoblot analysis. (F) Percentage of viable in vitro–differentiated erythroid cells from *Gpx4*$^{F/F}$, *Rip3*$^{-/-}$ (*Gpx4*$^{F/F}$Rip3$^{\Delta}$), *Rosa26-Cre*ER^{T2}/*Gpx4*$^{F/F}$ (*Gpx4*$^{\Delta}$), and *Rip3*$^{-/-}$/*Rosa26-Cre*ER^{T2}/*Gpx4*$^{F/F}$ (*Gpx4*$^{\Delta}$Rip3$^{\Delta}$) 48 hours after the induction of deletion. Data are mean ± SE; n ≥ 8; ****P* < .001 by ANOVA/Bonferroni. (G) Flow cytometry analysis of in vitro–cultured erythroid cells 36 hours after the 4-OHT treatment to analyze necrotic cells (AnnexinV^{-}PI^{+}). Data are mean ± SE; n ≥ 4; **P* < .05 by ANOVA/Bonferroni. (H) Deletion of *Rip3* significantly improved the formation of erythroid *o*-dianisidine–positive *Gpx4*$^{\Delta}$ colonies, similar to α-Toc supplementation. Data are mean ± SE; n ≥ 3; **P* < .05, ***P* < .01, ****P* < .001 by ANOVA/Bonferroni. ANOVA, analysis of variance.

increased dramatically in the spleen but to a lesser extent in the bone marrow (see supplemental Figure 1, available on the *Blood* Web site). Notably, serum interleukin 6 and double-stranded DNA antibody levels were unaltered, ruling out systemic inflammation or autoimmunity (supplemental Figure 2). The mice were monitored for 6 months after the induction of the deletion.

To determine whether increased lipid peroxidation and ROS accumulation in peripheral erythrocytes (Figure 2A-B) triggered their premature death, we determined the half-life of biotin-labeled erythrocytes (Ter119^{+}). Although turnover of peripheral Gpx4$^{\Delta}$ mature erythrocytes remained unaltered as compared to littermate controls (Figure 2C), the number of reticulocytes steadily increased within 4 weeks (Figure 2D). However, this was paralleled by massive cell death in spleen determined by TUNEL, and flow cytometry confirmed the increased number of PI^{+}CD71^{+} *Gpx4*$^{\Delta}$ cells in spleen and bone marrow (Figure 2E-H). The consequences of increased erythroid precursor death became even more apparent in the in vitro erythroid colony formation assay because formation of red colonies was nearly completely abolished in *Gpx4*$^{\Delta}$ bone marrow. However, colony formation could be significantly improved in the presence of α-tocopherol, the most prominent member of the vitamin E family (Figure 2I), recapitulating the phenotype of *Gpx4* deficiency in fibroblasts, neurons, kidney tubule cells, and endothelial cells.[12,17,33]

Vitamin E is essential for the compensatory increase in reticulocyte numbers in the absence of Gpx4

Recently, it was shown that the high vitamin E content typically present in regular animal chow (55-135 mg/kg) can partially compensate for *Gpx4* loss in endothelial cells in vivo.[33] To examine whether this was also the case during reticulocyte maturation, and to restrict *Gpx4* deletion to the hematopoietic system, we performed adoptive transfer experiments using bone marrow derived from *Gpx4*$^{F/F}$ or *Gpx4*$^{\Delta}$ mice. Five weeks after transplant, mice were kept on a vitamin E–depleted diet (7 mg/kg) until the end of the experiment; 8 weeks after transplant, the deletion was induced via poly(I:C) (Figure 3A). The mice were euthanized 3 weeks after the induction of the deletion. Upon the additional loss of vitamin E, red blood cell parameters were substantially lower (Figure 3B-D), whereas spleen size and EPO levels further increased (Figure 3F-G). However, dietary vitamin E depletion caused a significant decrease in reticulocyte numbers in mice that had received *Gpx4*$^{\Delta}$ bone marrow compared to controls (Figure 3E), supporting the notion that under these conditions, anemia could no longer be compensated.

Loss of Gpx4 triggers necroptosis

To further examine Gpx4 function in prevention of early erythroid cell death, we employed an erythrocyte maturation model that allows analysis of erythrocyte development ex vivo.[31] To initiate erythropoiesis, lineage-negative bone marrow cells derived from tamoxifen-inducible *Rosa26-CreER*^{T2}/*Gpx4*$^{F/F}$ mice[34] were cultured in the presence of

From www.bloodjournal.org by guest on January 11, 2016. For personal use only.

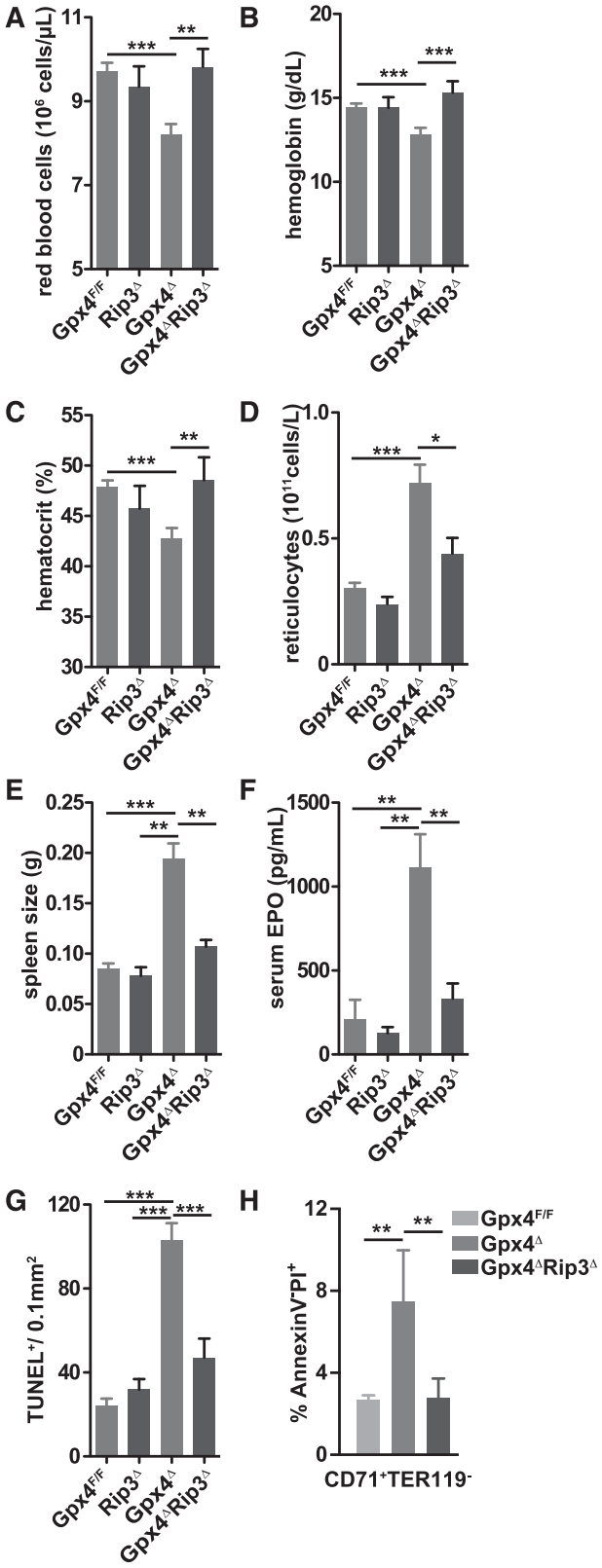

Figure 5. Genetic deletion of *Rip3* normalizes red cell parameters and rescues anemia. Normalization of red blood cell counts (A), hemoglobin levels (B), and hematocrit (C), and reduction of reticulocyte numbers (D). Enlarged spleens (E) and elevated serum EPO levels (F) in *Gpx4*$^{\Delta}$ mice are normalized upon deletion of *Rip3*. Data are mean ± SE; n ≥ 9. (G) Quantification of TUNEL^{+} cells in spleen sections. (H) Flow cytometry analysis of AnnexinV^{-}PI^{+} erythroid progenitor cells in the spleen. Data are mean ± SE; n ≥ 4. *$P < .05$, **$P < .01$, ***$P < .001$ by ANOVA/Bonferroni.

EPO, and 4-OHT was added 24 hours later to induce loss of *Gpx4*. Upon *Gpx4* deletion, the number of viable erythroid cells significantly decreased within 24 hours compared to *Gpx4*$^{F/F}$ control cells (Figure 4A-B,D), which could be prevented by α-tocopherol supplementation as expected (Figure 4D). Flow cytometric analysis confirmed increased cell death (PI^{+} cell number) in *Gpx4*-deficient CD71^{+}/Ter119^{+} cells (data not shown). Recently, Gpx4 has been described as an important regulator of ferroptosis.[14] To investigate the mechanism of cell death we have targeted variable regulatory elements of programmed cell death pathways (Figure 4C). Surprisingly, ferroptosis inhibition using the small inhibitor Fer-1 did not prevent cell death in *Gpx4*$^{\Delta}$ erythroid cultures and even reduced the viability of control cells, whereas erastin- and RLS3-induced ferroptosis was completely rescued in control cells and only partially rescued in *Gpx4*$^{\Delta}$ cells using the same concentration (supplemental Figure 3A). Similarly to Fer-1, another specific ferroptosis inhibitor, Lip-1, as well as the iron chelator DFO did not prevent cell death but reduced the number of control cells. Moreover, apoptosis blockade using the pan-caspase inhibitor zVAD also did not improve survival of *Gpx4*$^{\Delta}$ erythroid precursors. However, the RIP1 kinase inhibitor nec-1 normalized cell numbers, suggesting that *Gpx4*$^{\Delta}$ erythroid cell death was triggered by necroptosis. Yet, block of TNF signaling by recombinant soluble TNFR2 (etanercept) had no effect. Because it was recently demonstrated that due to off-target effects, nec-1 can prevent death of *Gpx4*-deficient fibroblasts even in the absence of RIP1,[17] we aimed to confirm the contribution of necroptosis by genetic ablation of *Rip3*, the upstream kinase responsible for mixed-lineage kinase domain–like protein phosphorylation.[35] To this end, we generated *Gpx4*$^{\Delta}$/*Rip3*$^{-/-}$ compound mutants. Loss of Gpx4 and RIP3 expression was confirmed by immunoblot analysis (Figure 4E) and, indeed, *Rip3* deletion prevented *Gpx4*$^{\Delta}$ erythroid cell death (Figure 4F). Flow cytometry confirmed normalization of PI^{+} CD71^{+}/Ter119^{+} cells (Figure 4G), and the number of red colonies was significantly increased in colony assays using bone marrow from *Gpx4*$^{\Delta}$/*Rip3*$^{-/-}$ compound mutants (Figure 4H). In line with these findings, deletion of *Rip3* also prevented anemia in *Gpx4*$^{\Delta}$ mice in vivo. All red cell parameters were normalized (Figure 5A-C), and the number of circulating reticulocytes was significantly decreased in *Gpx4*$^{\Delta}$/*Rip3*$^{-/-}$ mice (Figure 5D). In parallel, both spleen size and serum EPO levels were normalized upon loss of *Rip3* in *Gpx4*$^{\Delta}$ mice (Figure 5E-F). Accordingly, the increased number of TUNEL^{+} cells in *Gpx4*$^{\Delta}$ spleen was significantly reduced in *Gpx4*$^{\Delta}$/*Rip3*$^{-/-}$ double mutants (Figure 5G), which could be further confirmed by flow cytometry (Figure 5H). Collectively, the data support the notion that erythroid cells are undergoing RIP3-dependent necroptosis upon oxidative stress caused in the absence of *Gpx4*. Although Fer-1 addition reduced ROS accumulation and lipid peroxidation to a significant degree, both parameters were still higher in *Gpx4*$^{\Delta}$ cells compared to control cells (supplemental Figure 3B-C), which sufficed to stabilize RIP1 and RIP3 (supplemental Figure 3D), explaining ROS-induced necroptosis, even in the presence of Fer-1.

Necroptosis in Gpx4-deficient erythroid cells is triggered independently of TNF-α, CD95, or PARP

Necroptosis is an alternative form of programmed cell death usually associated with elevated levels of ROS.[22,36] Apart from Fas or certain Toll-like–receptor engagement, TNFR signaling is one of the best-characterized triggering events leading to mitochondrial ROS production and necroptosis when caspase 8 is inhibited.[23] Notably, despite having a profound effect on cell survival, *Rip3* deletion did not prevent

From www.bloodjournal.org by guest on January 11, 2016. For personal use only.

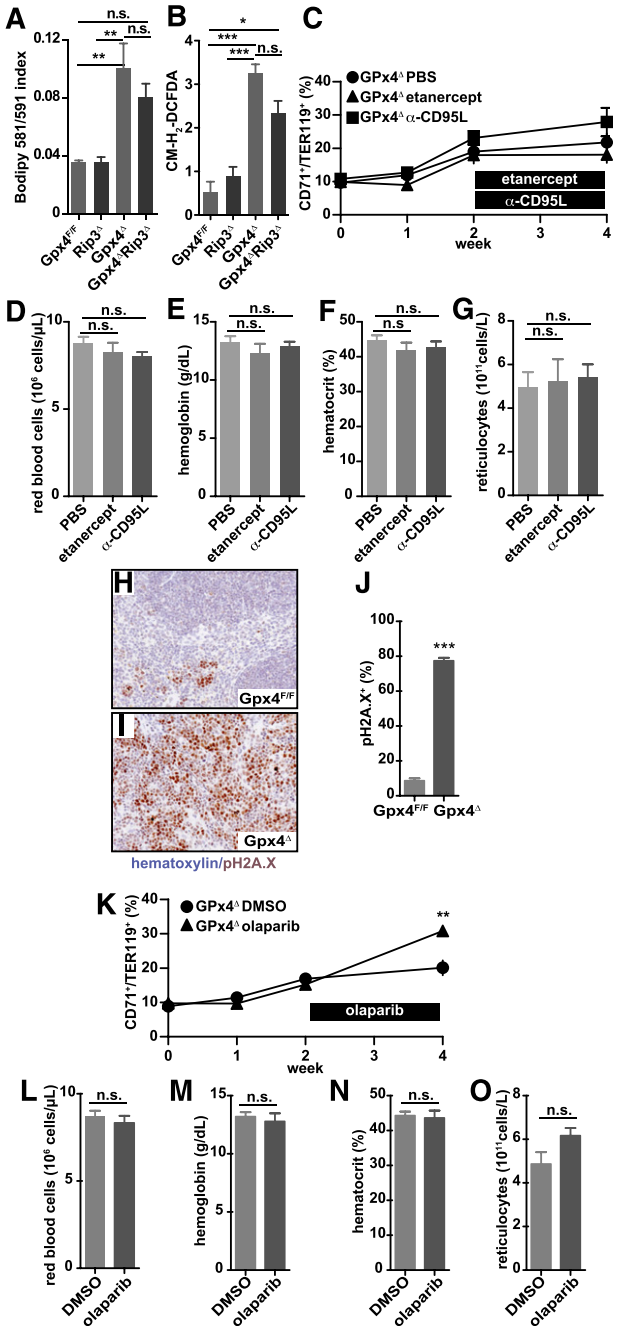

Figure 6. Necroptosis in *Gpx4*$^{\Delta}$ mice is triggered independently of TNFR or CD95 engagement and PARP activation. Lipid peroxidation (A) and ROS accumulation (B) in peripheral blood erythroid cells (TER119^{+}) are not significantly affected upon *Rip3* deletion. Data are mean ± SE; n ≥ 4; **P* < .05, ***P* < .01, ****P* < .001 by ANOVA/Bonferroni. The number of peripheral CD71^{+}/TER119^{+} cells remains unaffected (C), and there is no change in red blood cell counts (D), hemoglobin levels (E), hematocrit (F), and reticulocyte counts (G) in *Gpx4*$^{\Delta}$ mice when treated with etanercept (5 mg/kg) or anti-CD95L neutralizing antibody (50 µg) for 2 weeks. Data are mean ± SE; n ≥ 5. Immunohistochemistry of phospho-H2Ax (pH2Ax) and nuclear counterstain hematoxylin in the spleen (H-I) and the quantification of phospho-H2Ax^{+} foci (J). Image acquisition was performed using a Zeiss Axio Imager M2 with a 20×/0.5 EC Plan Neofluar objective (magnification ×200). Data are mean ± SE; n ≥ 3; ****P* < .001 by Student *t* test. The number of peripheral CD71^{+}/TER119^{+} cells remains unaffected (K), and there is no change in red blood cell counts (L), hemoglobin levels (M), hematocrit (N), and reticulocyte counts (O) in *Gpx4*$^{\Delta}$ mice when treated with the PARP inhibitor olaparib (5 mg/kg) for 2 weeks. Data are mean ± SE; n ≥ 5. DMSO, dimethylsulfoxide; PBS, phosphate-buffered saline.

accumulation of lipid peroxides and ROS in peripheral erythroid cells of *Gpx4*$^{\Delta}$ mice (Figure 6A-B), demonstrating that elevated lipid peroxidation and ROS levels per se are not sufficient to induce cell death upon *Gpx4* deletion. Surprisingly, etanercept did not prevent cell death in *Gpx4*-deficient erythroid cells ex vivo (Figure 4D). In line with these findings, treatment of *Gpx4*$^{\Delta}$ mice with etanercept did not normalize hemoglobin levels or reticulocyte counts (Figure 6C-G; supplemental Figure 4A). Moreover, a neutralizing antibody against CD95L at concentrations that sufficiently block respective signaling in vivo (supplemental Figure 4B-D) also did not normalize anemia or compensatory reticulocytosis (Figure 6C-G), excluding the role of both TNFR and FAS signaling as upstream events in necroptosis of *Gpx4*-deficient erythroid cells. Furthermore, despite a marked accumulation of phospho-H2A.X^{+} foci in the spleens of *Gpx4*$^{\Delta}$ mice (Figure 6H-J), PARP inhibition, which is known to block genotoxic stress–triggered necroptosis,[23] did not prevent anemia (Figure 6K-O; Figure 4E-G). Collectively, these data suggested that necroptosis was triggered independently of the classical activation pathways. To test whether loss of *Gpx4* led to the formation of the necrosome, we performed immunoprecipitation assays using protein lysates from in vitro–differentiated erythroid cells. Indeed, 4-OHT–induced *Gpx4* loss triggered the interaction of caspase 8 and RIP1; however, we were not able to detect any recruitment of FADD to this complex (Figure 7A). Yet, FADD was sufficiently recruited when necroptosis was triggered by TNF-α in the absence of caspase and TAK activity in the presence of Gpx4 (Figure 7A), supporting the notion that Gpx4-dependent necroptosis in erythroid cells occurred independently of TNF-α activation. Caspase 8 functions as an important inhibitor of the necrosome, being responsible for direct cleavage of RIP1 and RIP3[22] and of the RIP1-activating deubiquitinase, CYLD.[37] Thus, lack of caspase 8 function is associated with induction of necroptosis. Therefore, we reasoned that caspase 8 function might be impaired in *Gpx4*$^{\Delta}$ cells despite its recruitment and interaction with RIP1. This was confirmed, because cleavage of caspase 8 was impaired in *Gpx4*$^{\Delta}$ in vitro–differentiated erythrocytes when treated with TNF-α in the presence of the TAK1 inhibitor 5Z-7-oxozeaenol (TAKi) (Figure 7B). Shifting the redox potential toward oxidation has recently been demonstrated to decrease caspase 1 activity by transient glutathionylation.[38] To examine whether the increased ROS production caused by *Gpx4* deficiency might similarly affect caspase 8 function in *Gpx4*$^{\Delta}$ cells, we checked the glutathione state in CD71^{+}/Ter119^{+} erythroid progenitor cells isolated from bone marrow. As expected, *Gpx4* loss caused a dramatic increase in GSSG, leading to a decrease in the GSH/GSSG ratio (Figure 7C-D). Moreover, when the CD71^{+}/Ter119^{+} erythroid progenitor cells were loaded with BioGEE to precipitate glutathionylated proteins, immunoblot analysis of caspase 8 showed a marked glutathionylation in *Gpx4*$^{\Delta}$ cells compared to control cells (Figure 7E). Consequently, in in vitro–cultured progenitor cells, DTT prevented necrotic cell death and prevented caspase 8 inhibition (Figure 7F-G), yet this was not due to DTT-dependent inhibition of lipid peroxidation or ROS accumulation (Figure 7H-I). Collectively, these results indicate that in *Gpx4*$^{\Delta}$ cells, although caspase 8 is readily recruited to the necrosome, its functional impairment due to glutathionylation results in necrotic cell death (Figure 7J).

Discussion

Erythrocytes are well equipped with a variety of antioxidant systems to scavenge oxidative stress. So far, Gpx4, one of the most important

From www.bloodjournal.org by guest on January 11, 2016. For personal use only.

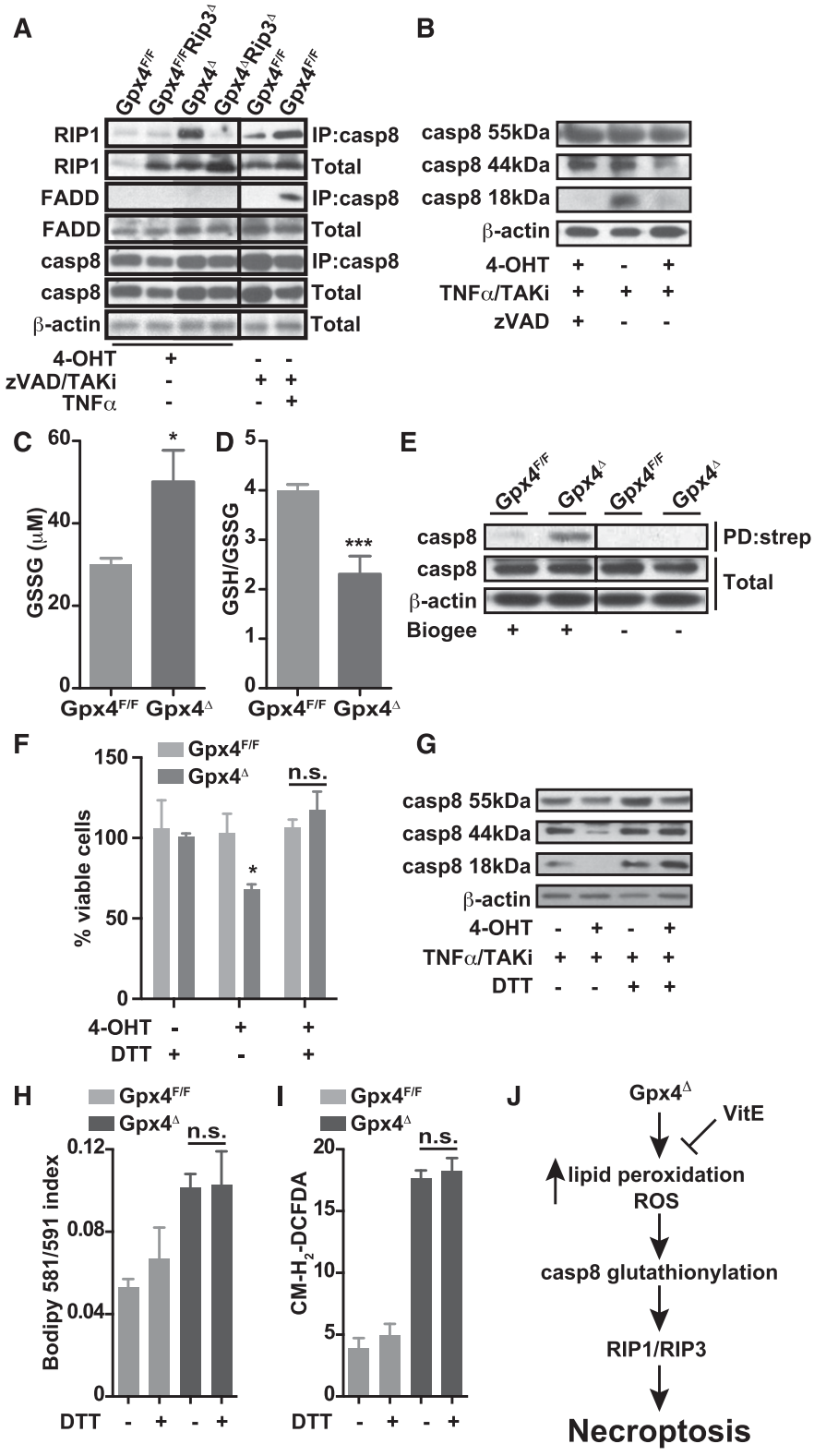

Figure 7. Caspase 8 is inactivated in *Gpx4*-deficient cells. (A) Immunoprecipitation of caspase 8 (IP:casp8) and immunoblot analysis of RIP1 and FADD in in vitro erythroid cultures treated with 4-OHT for 36 hours. Classical activation of necroptosis using zVAD/TAKi/TNF-α treatment in wild-type in vitro–cultured erythroid cells shows a strong interaction of caspase 8 with RIP1 and FADD upon 2 hours of stimulation. (B) Cleavage of caspase 8 (casp8) is blocked in in vitro–cultured *Gpx4*$^{\Delta}$ erythroid cells 36 hours after 4-OHT treatment, determined by immunoblot of caspase 8 when stimulated 2 hours with TNF-α in the presence of the TAK1 inhibitor 5Z-7-oxozeaenol (TAKi), whereas zVAD treatment completely inhibits caspase 8 cleavage. Concentration of GSSG (C) and the GSH/GSSG ratio (D) in peripheral blood cells of *Gpx4*$^{\Delta}$ mice and control littermates. (E) Detection of glutathionylated caspase 8 in peripheral CD71^{+}/TER119^{+} cells from *Gpx4*$^{\Delta}$ mice. Cells were loaded with BioGEE, and immunoblot analysis was performed after immunoprecipitation with streptavidin (PD:strep). Data shown is representative of 4 independently analyzed mice of each genotype. DTT supplementation rescues cell death in erythroid cells (F) and restores caspase 8 cleavage upon TNF-α stimulation (G). DTT treatment does not inhibit lipid peroxidation (H) or ROS accumulation (I) in cultured erythroid cells of either genotype. (J) Our model proposes that in the absence of Gpx4, lipid peroxides and ROS can act as signaling molecules upstream of the necrosome independently of TNFR/FAS signaling. Loss of Gpx4 in the erythroid lineage leads to inactivation of caspase 8 via glutathionylation. ROS and lipid peroxides activate the RIP1/RIP3–containing necrosome and trigger necroptotic cell death. The presence of vitamin E (VitE) can compensate for Gpx4 deficiency.

mammalian redox enzymes, has not been considered to be part of this finely tuned antioxidant defense system in this cell lineage. Here, we show that Gpx4 plays an important role in scavenging ROS and lipid hydroperoxides in the erythroid lineage. Loss of Gpx4 causes erythroid precursor cell death, which results in the development of anemia. However, this can be partially compensated for in the presence of exogenous vitamin E, whereas in the absence of vitamin E supplementation, compensatory reticulocytosis is completely impaired. Thus, vitamin E acts as the compensating ROS scavenger and provides a back-up system for Gpx4 in vivo, as it has recently been suggested in endothelial cells.[33] Similar kinetics of biotin-labeled Ter119^{+} cells underscore the notion that *Gpx4*$^{\Delta}$ mice do not develop

From www.bloodjournal.org by guest on January 11, 2016. For personal use only.

hemolytic anemia, but rather are characterized by insufficient erythropoiesis.

Lipid peroxidation, ROS formation, and induction of necrosis have been linked by several groups[39-42] to an increase in redox-active iron, the so-called intracellular labile iron pool, and to an increase in lysosomal iron.[43] Recently, a novel form of cell death, termed ferroptosis, has been described. Ferroptosis is triggered by the lethal oncogenic Ras-selective small molecule erastin in cancer cells in an iron-dependent fashion and could not be inhibited by nec-1.[15] In fact, recent data suggested an important role of Gpx4 for the survival of T cells and renal tubular cells by preventing ferroptosis.[14] In this study, we provide evidence that in erythroid cells, Gpx4 instead suppresses Rip3-dependent necroptosis. Although the cell death mechanisms seems to vary between different cell types, Gpx4 is clearly a vital element for the homeostasis of hematopoietic cells via regulating the cellular redox balance and thus inhibiting cell death. However, it is not clear to what extent these different cell death pathways are overlapping or interchangeable based on genetic or environmental alterations. There are several studies demonstrating the complex interchange between death mechanisms upon genetic alterations of the regulating elements such as FADD, caspase 8, RIP1, and RIP3.[44-46]

Different subcellular sources of ROS have been described to contribute to TNF-α–induced necrosis in L929 cells. ROS produced at complex I and II in the mitochondrial electron transport chain play a crucial role in the execution of TNF-α–induced necrosis.[39] Antioxidants, as well as iron chelators, were able to rescue L929 cells from TNF-α–induced necrosis, implying that the intracellular labile iron pool and ROS generated through the Fenton reaction play an important role in the execution of cell death.[39] Engagement of TNFR1 by TNF induces formation of a signaling complex consisting of TNFR1-associated DEATH domain protein, RIP1, and the reduced NAD phosphate oxidase Nox1 that leads to Nox1 activation, oxygen production at the plasma membrane, long-term JNK1 activation by cytoplasmic ROS, and necrotic cell death.[40,41] Furthermore, TNF-α can stimulate ROS formation by favoring JNK1-dependent degradation of the ubiquitous iron-binding protein ferritin, leading to an increase in redox-active iron.[42] Of importance, however, in all instances, ROS and lipid peroxidation have been considered essential downstream effectors of RIP1/RIP3–dependent signaling. Yet, we show here that the deletion of *Rip3* prevents anemia induced by *Gpx4* deletion without inhibiting lipid peroxidation and ROS production, thereby suggesting that lipid peroxides and ROS can act as signaling molecules upstream of the necrosome independently of TNF-α stimulation. However, this finding does not rule out the possibility that ROS may also play an important role as effectors of necrotic cell death downstream of the RIP/RIP3 signaling complex. Indeed, the slight reduction in lipid peroxidation and ROS levels upon additional deletion of *Rip3* is possibly verifying the role of cellular ROS induction during the execution of RIP3-dependent necroptosis, even though the necroptosis in the case of Gpx4 deficiency is independent of TNFR signaling. Consistent with a lack of FADD recruitment to the necrosome complex, TNF-α, FAS ligand, and DNA damage–dependent PARP1 activation do not play a role in the induction of Gpx4-deficient cell death. Thus, we propose an as-yet-unrecognized unconventional pathway for the initiation of necroptosis that is independent of TNFR and FAS engagement. One important prerequisite seems to be the functional inactivation of caspase 8, possibly by glutathionylation, in *Gpx4*-deficient cells. Similarly, glutathionylation has been proposed to be involved in the regulation of caspase 1 and caspase 3.[38,47] Because glutathionylation is a direct consequence of oxidation, our findings may nevertheless also be relevant for classical TNF-α–dependent necrosome activation, because ROS that are formed downstream of RIP1/RIP3 may interfere with caspase 8 activity and therefore fuel a feed-forward loop.[48] Furthermore, we cannot rule out that caspase 8 is also inhibited by direct oxidation of the active-site cysteine.[49,50]

In conclusion, our data provide direct genetic evidence that Gpx4 can act as a yet-unrecognized regulator of RIP3-dependent necroptosis in a cell type–dependent manner. The underlying explanation for this particular cell type–specific difference is currently unknown, but it will be important to identify the factors that determine the cell death mechanism (ie, necroptosis vs ferroptosis), when Gpx4 is not functional.

Acknowledgments

The authors thank Natalia Delis, Christin Danneil, Eva Rudolf, Kerstin Burmeister, and Saskia Ettl for expert technical assistance; Vishva Dixit and Kim Newton for providing *Rip3*$^{-/-}$ mice; and Markus Conrad for providing *Gpx4*$^{F/F}$ mice.

This work was supported in part by the Landesoffensive zur Entwicklung Wissenschaftlich-ökonomischer Exzellenz (LOEWE) Center for Cell and Gene Therapy Frankfurt (CGT, III L 4-518/17.004); institutional funds from the Georg-Speyer-Haus; and a grant from the European Research Council (ERC 281967) (F.R.G.).

Authorship

Contribution: Ö.C., Y.B.A., N.V., L.H., and P.S.H., performed and analyzed the experiments; T.S., G.W.B., and F.R.G. analyzed the experiments; S.G. and P.V. contributed to the analysis of cell death; G.W.B. and F.R.G. supervised and designed the experiments; and G.W.B., F.R.G., and Ö.C. wrote the manuscript.

Conflict-of-interest disclosure: The authors declare no competing financial interests.

Correspondence: Florian R. Greten, Institute of Tumor Biology and Experimental Therapy, Georg-Speyer-Haus, Paul-Ehrlich-Strasse 42-44, D-60596 Frankfurt, Germany; e-mail: greten@gsh.uni-frankfurt.de.

References

1. D'Autréaux B, Toledano MB. ROS as signalling molecules: mechanisms that generate specificity in ROS homeostasis. *Nat Rev Mol Cell Biol.* 2007; 8(10):813-824.
2. Vanden Berghe T, Vanlangenakker N, Parthoens E, et al. Necroptosis, necrosis and secondary necrosis converge on similar cellular disintegration features. *Cell Death Differ.* 2010; 17(6):922-930.
3. Fiers W, Beyaert R, Declercq W, Vandenabeele P. More than one way to die: apoptosis, necrosis and reactive oxygen damage. *Oncogene.* 1999; 18(54):7719-7730.
4. Beutler E, Luzzatto L. Hemolytic anemia. *Semin Hematol.* 1999;36(4 Suppl 7):38-47.
5. Johnson RM, Ho Y-S, Yu D-Y, Kuypers FA, Ravindranath Y, Goyette GW. The effects of disruption of genes for peroxiredoxin-2, glutathione peroxidase-1, and catalase on erythrocyte oxidative metabolism. *Free Radic Biol Med.* 2010;48(4):519-525.
6. Lee TH, Kim SU, Yu SL, et al. Peroxiredoxin II is essential for sustaining life span of erythrocytes in mice. *Blood.* 2003;101(12): 5033-5038.
7. Neumann CA, Krause DS, Carman CV, et al. Essential role for the peroxiredoxin Prdx1 in

From www.bloodjournal.org by guest on January 11, 2016. For personal use only.

erythrocyte antioxidant defence and tumour suppression. *Nature.* 2003;424(6948):561-565.

8. Kaushal N, Hegde S, Lumadue J, Paulson RF, Prabhu KS. The regulation of erythropoiesis by selenium in mice. *Antioxid Redox Signal.* 2011; 14(8):1403-1412.
9. Behne D, Kyriakopoulos A. Mammalian selenium-containing proteins. *Annu Rev Nutr.* 2001;21: 453-473.
10. Imai H, Hirao F, Sakamoto T, et al. Early embryonic lethality caused by targeted disruption of the mouse PHGPx gene. *Biochem Biophys Res Commun.* 2003;305(2):278-286.
11. Yant LJ, Ran Q, Rao L, et al. The selenoprotein GPX4 is essential for mouse development and protects from radiation and oxidative damage insults. *Free Radic Biol Med.* 2003;34(4):496-502.
12. Seiler A, Schneider M, Förster H, et al. Glutathione peroxidase 4 senses and translates oxidative stress into 12/15-lipoxygenase dependent- and AIF-mediated cell death. *Cell Metab.* 2008;8(3):237-248.
13. Ueta T, Inoue T, Furukawa T, et al. Glutathione peroxidase 4 is required for maturation of photoreceptor cells. *J Biol Chem.* 2012;287(10): 7675-7682.
14. Matsushita M, Freigang S, Schneider C, Conrad M, Bornkamm GW, Kopf M. T cell lipid peroxidation induces ferroptosis and prevents immunity to infection. *J Exp Med.* 2015;212(4): 555-568.
15. Dixon SJ, Lemberg KM, Lamprecht MR, et al. Ferroptosis: an iron-dependent form of nonapoptotic cell death. *Cell.* 2012;149(5): 1060-1072.
16. Yang WS, SriRamaratnam R, Welsch ME, et al. Regulation of ferroptotic cancer cell death by GPX4. *Cell.* 2014;156(1-2):317-331.
17. Friedmann Angeli JP, Schneider M, Proneth B, et al. Inactivation of the ferroptosis regulator Gpx4 triggers acute renal failure in mice. *Nat Cell Biol.* 2014;16(12):1180-1191.
18. Bergsbaken T, Fink SL, Cookson BT. Pyroptosis: host cell death and inflammation. *Nat Rev Microbiol.* 2009;7(2):99-109.
19. Christofferson DE, Yuan J. Necroptosis as an alternative form of programmed cell death. *Curr Opin Cell Biol.* 2010;22(2):263-268.
20. Wang Y, Dawson VL, Dawson TM. Poly(ADP-ribose) signals to mitochondrial AIF: a key event in parthanatos. *Exp Neurol.* 2009;218(2):193-202.
21. Degterev A, Hitomi J, Germscheid M, et al. Identification of RIP1 kinase as a specific cellular target of necrostatins. *Nat Chem Biol.* 2008;4(5): 313-321.
22. Vandenabeele P, Galluzzi L, Vanden Berghe T, Kroemer G. Molecular mechanisms of necroptosis: an ordered cellular explosion. *Nat Rev Mol Cell Biol.* 2010;11(10):700-714.
23. Han J, Zhong CQ, Zhang DW. Programmed necrosis: backup to and competitor with apoptosis in the immune system. *Nat Immunol.* 2011;12(12): 1143-1149.
24. Kaiser WJ, Upton JW, Long AB, et al. RIP3 mediates the embryonic lethality of caspase-8-deficient mice. *Nature.* 2011;471(7338):368-372.
25. Oberst A, Dillon CP, Weinlich R, et al. Catalytic activity of the caspase-8-FLIP(L) complex inhibits RIPK3-dependent necrosis. *Nature.* 2011; 471(7338):363-367.
26. Zhang H, Zhou X, McQuade T, Li J, Chan FK, Zhang J. Functional complementation between FADD and RIP1 in embryos and lymphocytes. *Nature.* 2011;471(7338):373-376.
27. Welz PS, Wullaert A, Vlantis K, et al. FADD prevents RIP3-mediated epithelial cell necrosis and chronic intestinal inflammation. *Nature.* 2011; 477(7364):330-334.
28. Bonnet MC, Preukschat D, Welz P-S, et al. The adaptor protein FADD protects epidermal keratinocytes from necroptosis in vivo and prevents skin inflammation. *Immunity.* 2011;35(4): 572-582.
29. Dillon CP, Oberst A, Weinlich R, et al. Survival function of the FADD-CASPASE-8-cFLIP(L) complex. *Cell Reports.* 2012;1(5):401-407.
30. Newton K, Sun X, Dixit VM. Kinase RIP3 is dispensable for normal NF-κBs, signaling by the B-cell and T-cell receptors, tumor necrosis factor receptor 1, and Toll-like receptors 2 and 4. *Mol Cell Biol.* 2004;24(4):1464-1469.
31. Shuga J, Zhang J, Samson LD, Lodish HF, Griffith LG. In vitro erythropoiesis from bone marrow-derived progenitors provides a physiological assay for toxic and mutagenic compounds. *Proc Natl Acad Sci USA.* 2007;104(21):8737-8742.
32. Kühn R, Schwenk F, Aguet M, Rajewsky K. Inducible gene targeting in mice. *Science.* 1995;269(5229):1427-1429.
33. Wortmann M, Schneider M, Pircher J, et al. Combined deficiency in glutathione peroxidase 4 and vitamin E causes multiorgan thrombus formation and early death in mice. *Circ Res.* 2013; 113(4):408-417.
34. Hameyer D, Loonstra A, Eshkind L, et al. Toxicity of ligand-dependent Cre recombinases and generation of a conditional Cre deleter mouse allowing mosaic recombination in peripheral tissues. *Physiol Genomics.* 2007;31(1):32-41.
35. Silke J, Rickard JA, Gerlic M. The diverse role of RIP kinases in necroptosis and inflammation. *Nat Immunol.* 2015;16(7):689-697.
36. Degenhardt K, Mathew R, Beaudoin B, et al. Autophagy promotes tumor cell survival and restricts necrosis, inflammation, and tumorigenesis. *Cancer Cell.* 2006;10(1):51-64.
37. O'Donnell MA, Perez-Jimenez E, Oberst A, et al. Caspase 8 inhibits programmed necrosis by processing CYLD. *Nat Cell Biol.* 2011;13(12): 1437-1442.
38. Meissner F, Molawi K, Zychlinsky A. Superoxide dismutase 1 regulates caspase-1 and endotoxic shock. *Nat Immunol.* 2008;9(8):866-872.
39. Schulze-Osthoff K, Bakker AC, Vanhaesebroeck B, Beyaert R, Jacob WA, Fiers W. Cytotoxic activity of tumor necrosis factor is mediated by early damage of mitochondrial functions. Evidence for the involvement of mitochondrial radical generation. *J Biol Chem.* 1992;267(8): 5317-5323.
40. Kamata H, Honda S, Maeda S, Chang L, Hirata H, Karin M. Reactive oxygen species promote TNFalpha-induced death and sustained JNK activation by inhibiting MAP kinase phosphatases. *Cell.* 2005;120(5):649-661.
41. Kim YS, Morgan MJ, Choksi S, Liu ZG. TNF-induced activation of the Nox1 NADPH oxidase and its role in the induction of necrotic cell death. *Mol Cell.* 2007;26(5):675-687.
42. Xie C, Zhang N, Zhou H, et al. Distinct roles of basal steady-state and induced H-ferritin in tumor necrosis factor-induced death in L929 cells. *Mol Cell Biol.* 2005;25(15):6673-6681.
43. Berndt C, Kurz T, Selenius M, Fernandes AP, Edgren MR, Brunk UT. Chelation of lysosomal iron protects against ionizing radiation. *Biochem J.* 2010;432(2):295-301.
44. Dannappel M, Vlantis K, Kumari S, et al. RIPK1 maintains epithelial homeostasis by inhibiting apoptosis and necroptosis. *Nature.* 2014; 513(7516):90-94.
45. Takahashi N, Vereecke L, Bertrand MJM, et al. RIPK1 ensures intestinal homeostasis by protecting the epithelium against apoptosis. *Nature.* 2014;513(7516):95-99.
46. Rickard JA, O'Donnell JA, Evans JM, et al. RIPK1 regulates RIPK3-MLKL-driven systemic inflammation and emergency hematopoiesis. *Cell.* 2014;157(5):1175-1188.
47. Pan S, Berk BC. Glutathiolation regulates tumor necrosis factor-alpha-induced caspase-3 cleavage and apoptosis: key role for glutaredoxin in the death pathway. *Circ Res.* 2007;100(2): 213-219.
48. Goossens V, De Vos K, Vercammen D, et al. Redox regulation of TNF signaling. *Biofactors.* 1999;10(2-3):145-156.
49. Borutaite V, Brown GC. Caspases are reversibly inactivated by hydrogen peroxide. *FEBS Lett.* 2001;500(3):114-118.
50. Hampton MB, Stamenkovic I, Winterbourn CC. Interaction with substrate sensitises caspase-3 to inactivation by hydrogen peroxide. *FEBS Lett.* 2002;517(1-3):229-232.

From www.bloodjournal.org by guest on January 11, 2016. For personal use only.

blood

2016 127: 139-148
doi:10.1182/blood-2015-06-654194 originally published online October 13, 2015

Glutathione peroxidase 4 prevents necroptosis in mouse erythroid precursors

Özge Canli, Yasemin B. Alankus, Sasker Grootjans, Naidu Vegi, Lothar Hültner, Philipp S. Hoppe, Timm Schroeder, Peter Vandenabeele, Georg W. Bornkamm and Florian R. Greten

Updated information and services can be found at:
http://www.bloodjournal.org/content/127/1/139.full.html

Articles on similar topics can be found in the following Blood collections
Red Cells, Iron, and Erythropoiesis (689 articles)

Information about reproducing this article in parts or in its entirety may be found online at:
http://www.bloodjournal.org/site/misc/rights.xhtml#repub_requests

Information about ordering reprints may be found online at:
http://www.bloodjournal.org/site/misc/rights.xhtml#reprints

Information about subscriptions and ASH membership may be found online at:
http://www.bloodjournal.org/site/subscriptions/index.xhtml

Blood (print ISSN 0006-4971, online ISSN 1528-0020), is published weekly by the American Society of Hematology, 2021 L St, NW, Suite 900, Washington DC 20036.
Copyright 2011 by The American Society of Hematology; all rights reserved.